

Two photon results from LEP



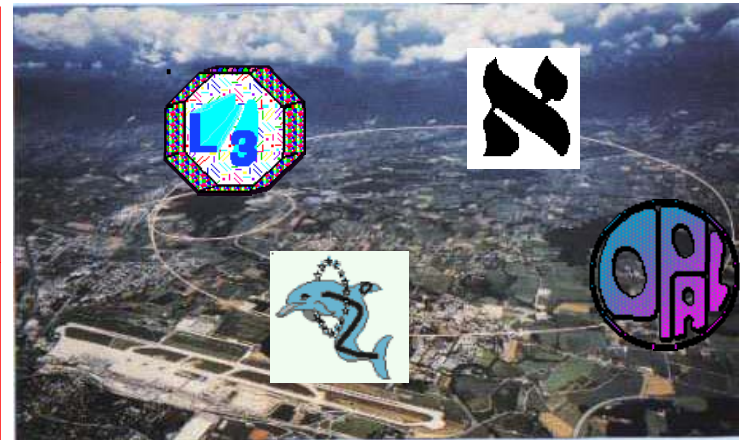
Mariusz Przybycień
AGH-UST Cracow



LEP: $e^+ e^-$ collisions at cms energies:
1989 - 1995: $\sqrt{s} = 91 \text{ GeV}$ (LEP1)
1996 - 2000: $\sqrt{s} = 161 - 209 \text{ GeV}$ (LEP2)

Experiments:

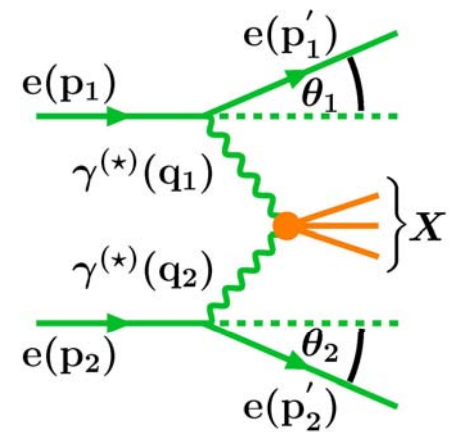
ALEPH, DELPHI, L3, OPAL



Study of two photon interactions through

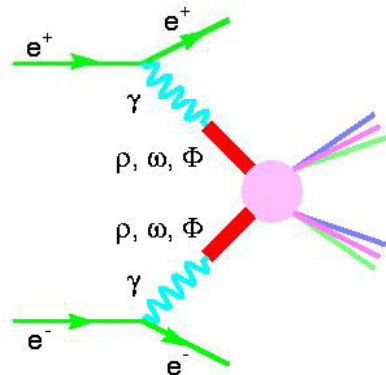
$$e^+ e^- \rightarrow e^+ e^- \gamma^{(*)} \gamma^{(*)} \rightarrow e^+ e^- X$$

- **Untagged ev.** - total cross section, jets production, heavy quarks, exclusive particle production
- **Single-tagged ev.** - QED and hadronic structure functions of the quasi-real photon
- **Double-tagged ev.** - dynamics of highly virtual photon collisions

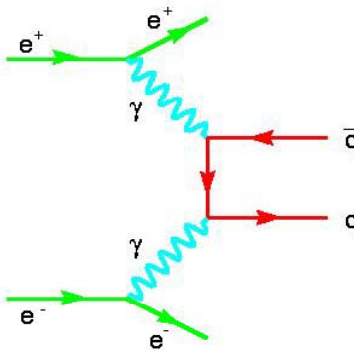


Total cross section for $\gamma\gamma \rightarrow$ hadrons

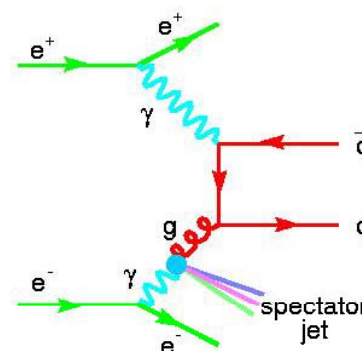
The following LO diagrams contribute to the process $\gamma\gamma \rightarrow$ hadrons:



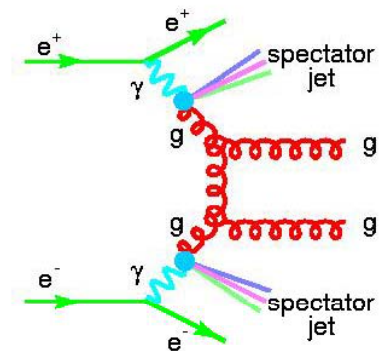
VMD



Direct

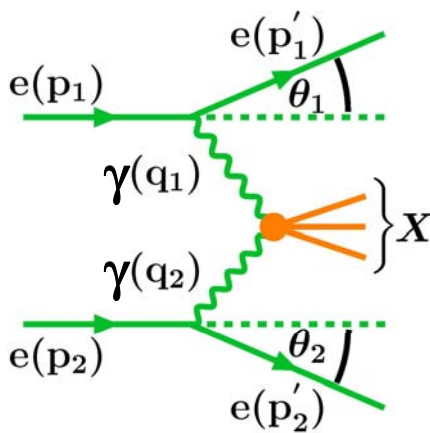


Single-resolved



Double-resolved

Kinematical variables for the process $\gamma\gamma \rightarrow$ hadrons:



$$s_{ee} = (p_1 + p_2)^2$$

$$Q_i^2 \equiv -q_i^2 = -(p_i - p'_i)^2 \approx 2E'_i E_b (1 - \cos \theta_i)$$

$$Q^2 \equiv \max(Q_1^2, Q_2^2) \quad P^2 \equiv \min(Q_1^2, Q_2^2)$$

$$W^2 \equiv W_{\gamma\gamma}^2 = (q_1 + q_2)^2 \approx (\sum_h E_h)^2 - (\sum_h \vec{p}_h)^2 = E_X^2 - \vec{p}_X^2$$

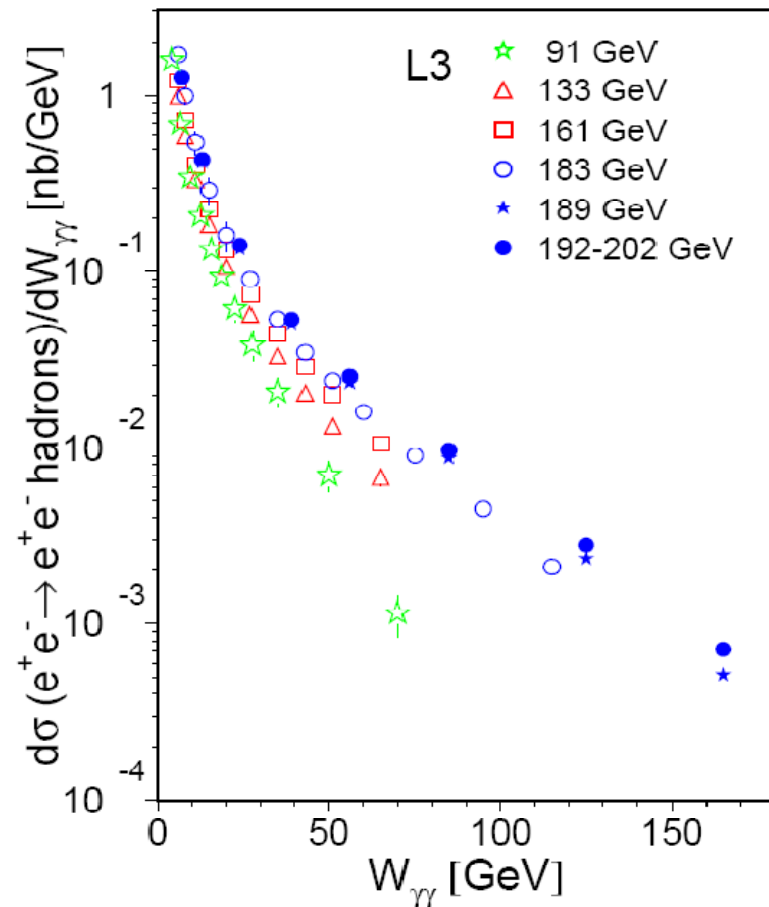
Total cross section for $\gamma\gamma \rightarrow \text{hadrons}$

- photon-photon scattering has the largest hadronic cross section at LEP2 energies
- in the framework of Regge theory $\sigma_{\gamma\gamma}$ is related to $\sigma_{\gamma p}$ and s_{hh} and a slow rise with $W_{\gamma\gamma}$ is predicted

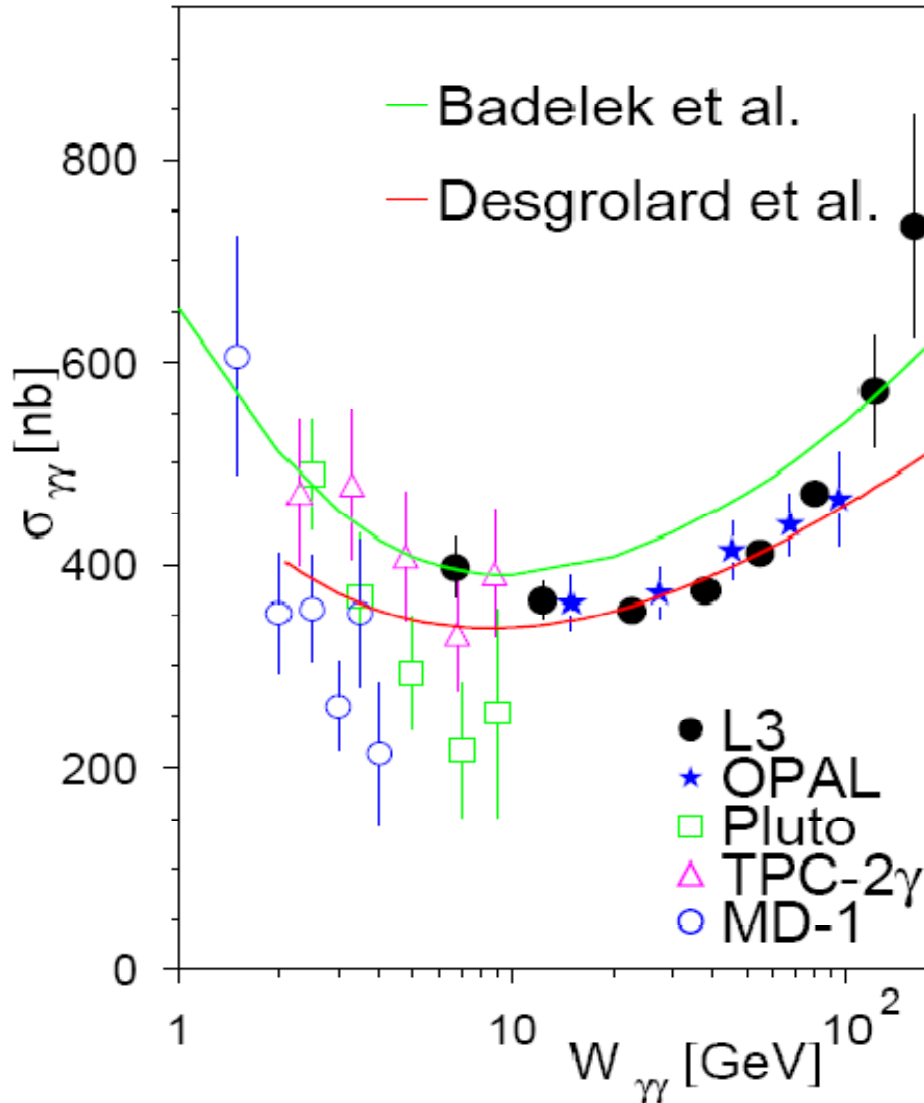
Measurement (L3, OPAL):

- first measure the differential cross section $d\sigma_{ee}/dW$ for the process: $e^+e^- \rightarrow e^+e^- + \text{hadrons}$
 - increasing with the beam energy
 - decreasing with $W_{\gamma\gamma}$ (effect of the $L_{\gamma\gamma}$)
- extract $\sigma_{\gamma\gamma}$ using the luminosity function $L_{\gamma\gamma}$ and form factors $F(Q^2)$ which describe the Q^2 dependence of the hadronic cross section

$$\frac{d\sigma_{ee}}{dW} = L_{\gamma\gamma} \otimes \sigma_{\gamma\gamma}$$



Total cross section for $\gamma\gamma \rightarrow$ hadrons



OPAL: $\sqrt{s} = 161 - 183 \text{ GeV}^2$
 $10 < W < 110 \text{ GeV}$

L3: $\sqrt{s} = 161 - 202 \text{ GeV}^2$
 $5 < W < 185 \text{ GeV}$

- Good agreement with previous measurements in the overlapping region
- Rise with W for $W > 10 \text{ GeV}^2$ which is characteristic for hadronic cross sections
- L3 data show steeper rise than expected for hadron-hadron or photon-proton cross sections.

Total cross section for $\gamma\gamma \rightarrow$ hadrons

OPAL fit: Regge parametrization with soft and hard pomeron:

$$\sigma_{\gamma\gamma}(W^2) = X_{1\gamma\gamma}(W^2)^{\varepsilon_1} + X_{2\gamma\gamma}(W^2)^{\varepsilon_2} + Y_{1\gamma\gamma}(W^2)^{-\eta_1}$$

fix reggeon term: $\eta_1 = 0.34$ oraz $Y_{1\gamma\gamma} = 320$ nb

results of the fit: $X_{2\gamma\gamma} = 0.5 \pm 0.2(\text{stat})_{-1.0}^{+1.5}(\text{sys})$ nb

what is consistent with zero (no hard pomeron)

results of the fit:

$$\varepsilon_1 = 0.101 \pm 0.004(\text{stat})_{-0.019}^{+0.025}(\text{sys})$$

$$X_{1\gamma\gamma} = 180 \pm 5(\text{stat})_{-32}^{+30}(\text{sys}) \text{ nb}$$

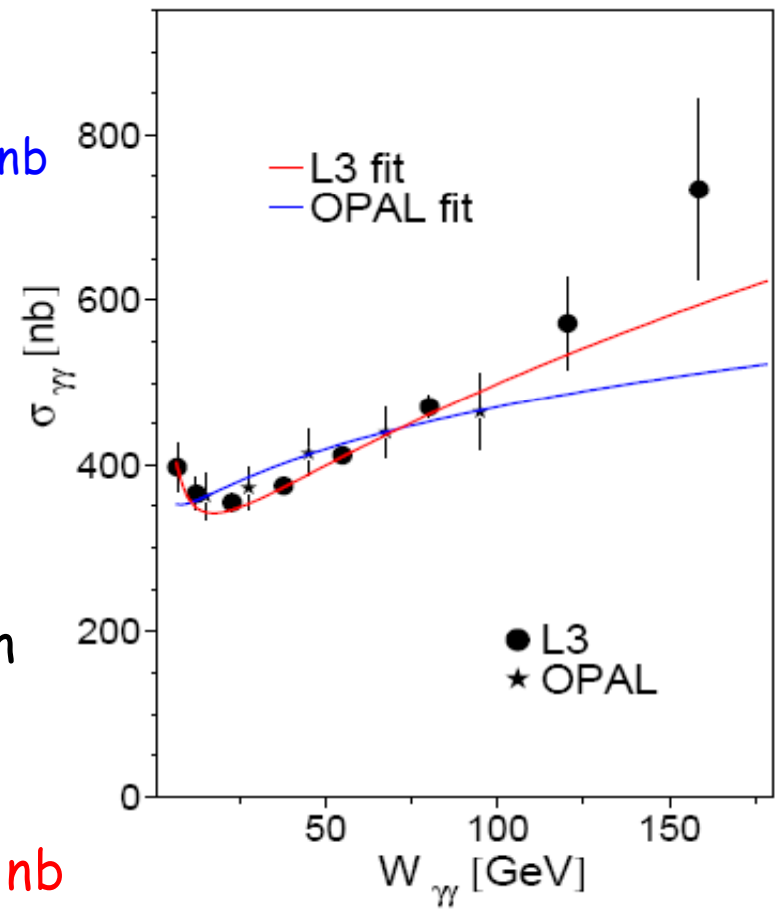
L3 fit:

Regge parametrization with soft pomeron

fix reggeon term: $\eta_1 = 0.358$

results of the fit: $\varepsilon_1 = 0.225 \pm 0.021$

$$X_{1\gamma\gamma} = 58 \pm 10 \text{ nb} \quad Y_{1\gamma\gamma} = 1020 \pm 146 \text{ nb}$$



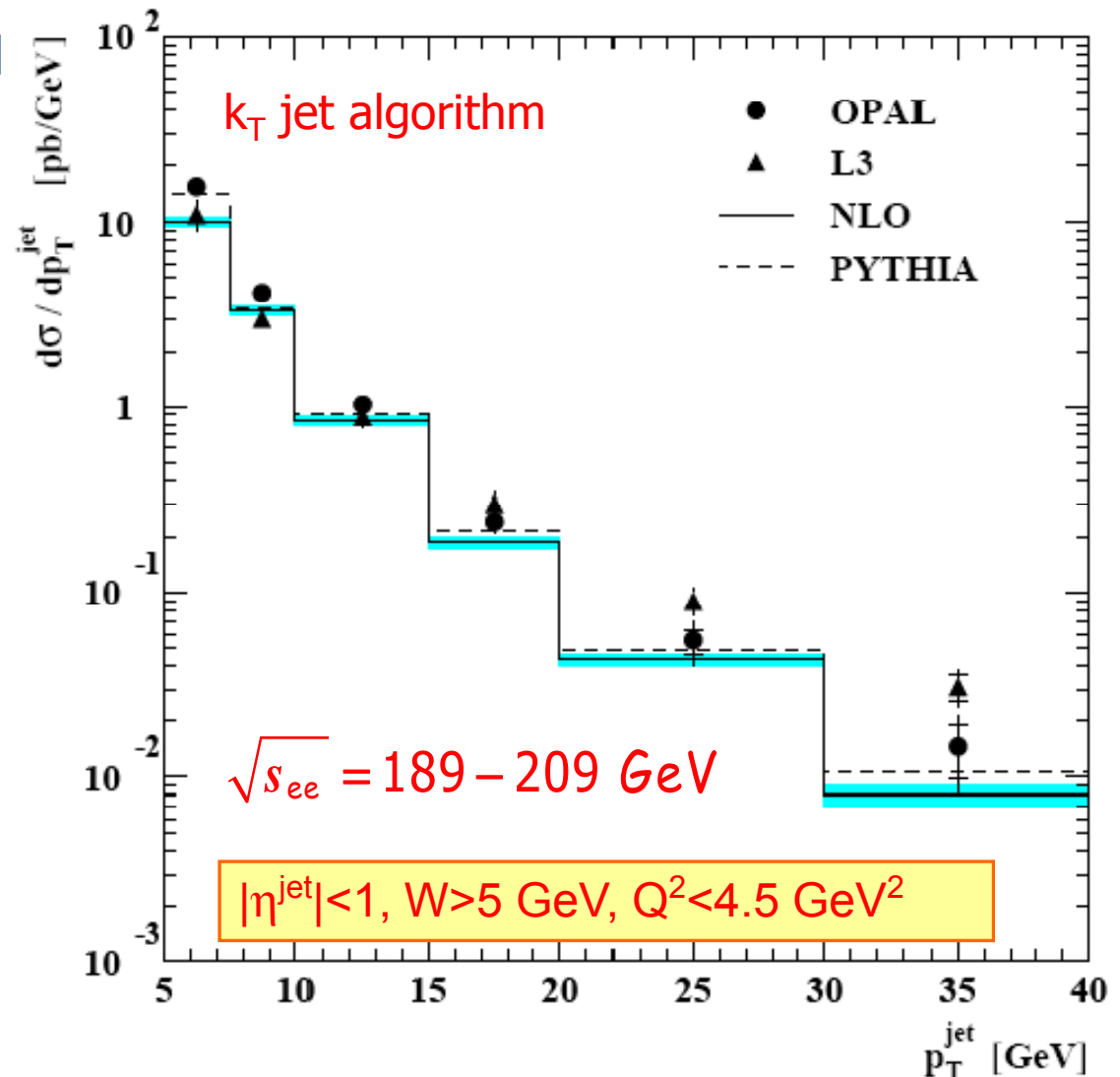
Inclusive jet cross section

NLO cross section calculated using QCD partonic cross sections in NLO for direct, single- and double-resolved processes convoluted with photon flux + hadronization corrections.

OPAL data well described by both Pythia and NLO.

Discrepancy in shape between L3 and NLO.

Disagreement between L3 and OPAL.



Di-jet cross production

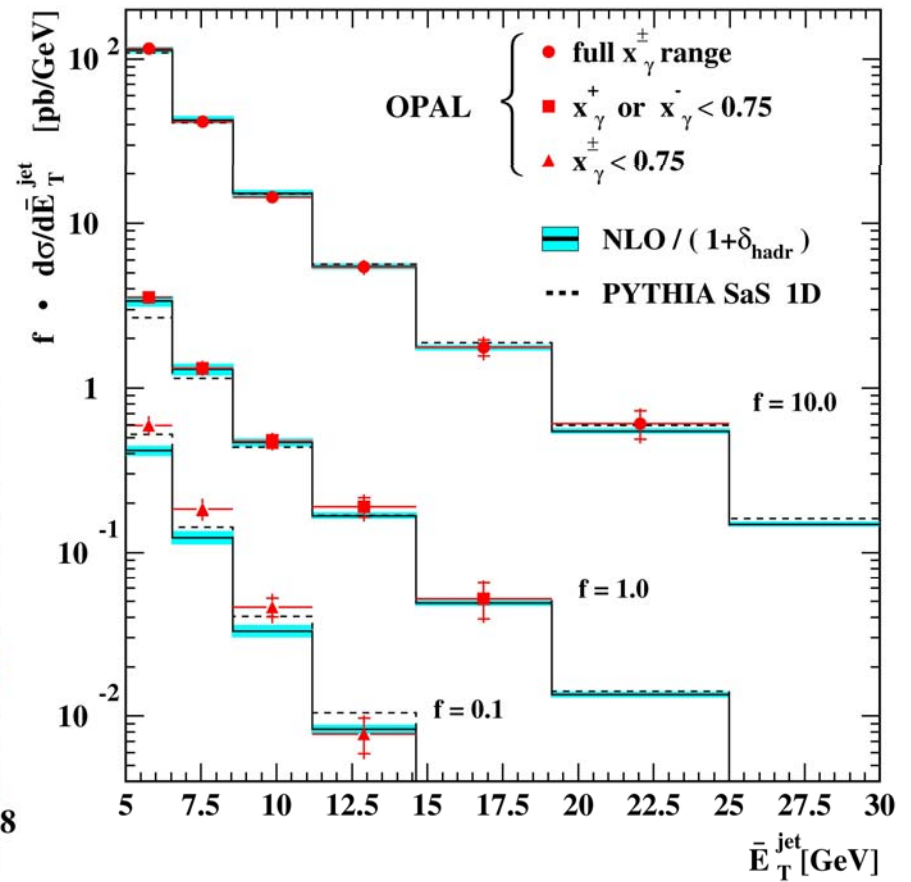
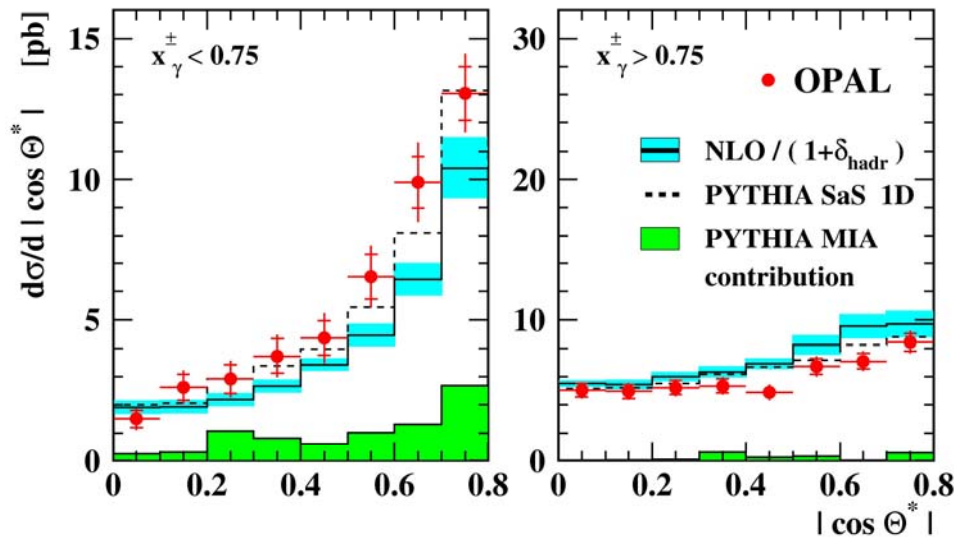
Experimentally, direct and double-resolved interactions can be clearly separated using the quantity:

The scattering angle θ^Σ in the two photon cms:

$$\cos \theta^* = \tanh \frac{\eta^{\text{jet1}} - \eta^{\text{jet2}}}{2}$$

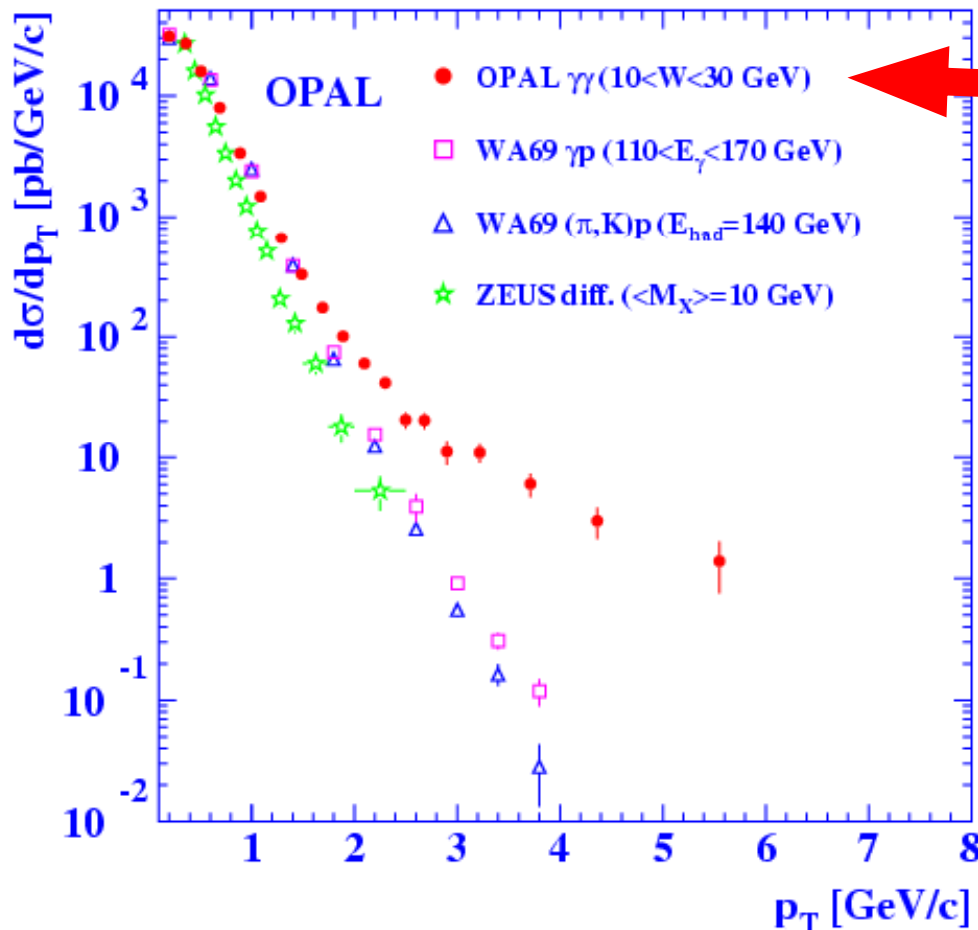
$$x_\gamma^\pm = \frac{\sum_{\text{jets}=1,2} (E \pm p_z)}{\sum_{\text{hadrons}} (E \pm p_z)}$$

NLO - contribution from underlying event which is largest at $x_\gamma^\pm < 0.75$ is not included!



Production of charged hadrons

Sensitivity to the structure of $\gamma\text{-}\gamma$ interactions without theoretical and experimental problems related to definition and reconstruction of jets.

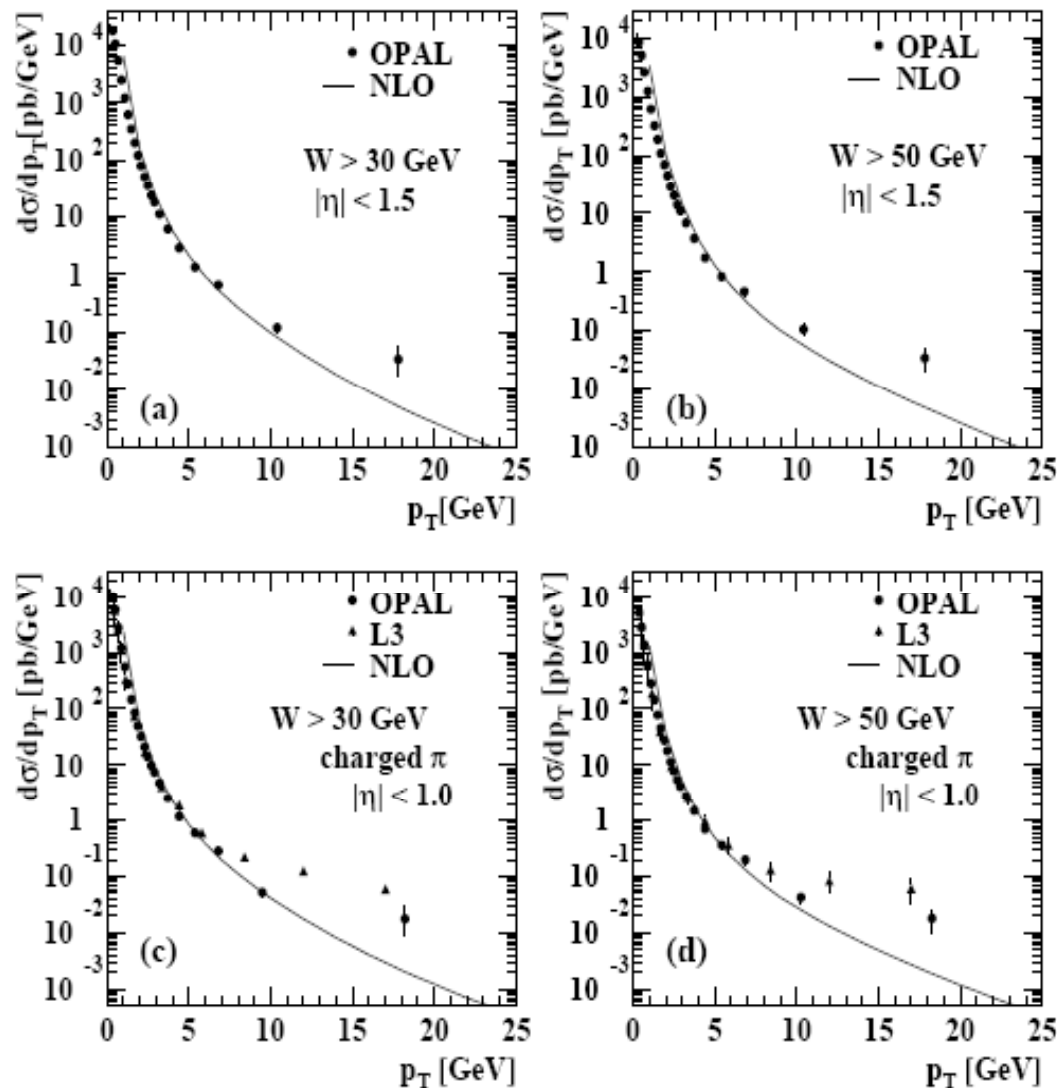


OPAL: $\sqrt{s_{ee}} = 161 - 172$ GeV

The spectrum of transverse momentum of charged hadrons in $\gamma\text{-}\gamma$ scattering is much harder than in the case of $\gamma\text{-}p$, $(\pi, K)\text{-}p$ and $\gamma\text{-}IP$.

This can be attributed to the direct component of the $\gamma\text{-}\gamma$ interactions.

Production of charged hadrons

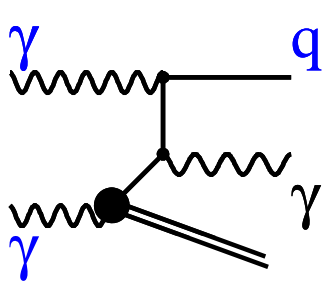


Differential cross sections measured by OPAL fall more rapidly towards high transverse momenta than those measured by L3, leading to a disagreement between the two experiments and to a better description of the OPAL data by NLO QCD.

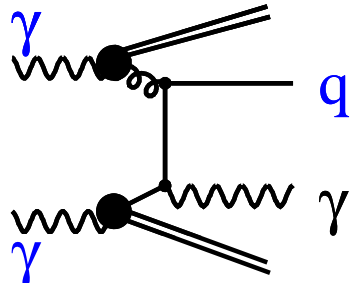
For the purpose of this comparison OPAL data have been scaled to reduced $|c|$ range and to the fraction of pions in all charged hadrons.

Isolated prompt photons

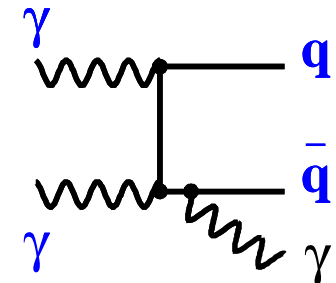
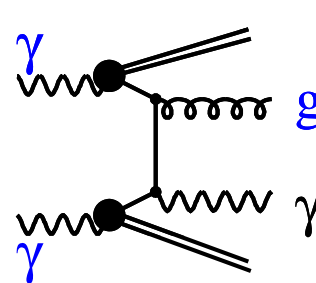
In LO only single and double resolved diagrams contribute to production of prompt photons $\gamma+\gamma \rightarrow \gamma+\text{hadrons}$:



Single-resolved



Double-resolved



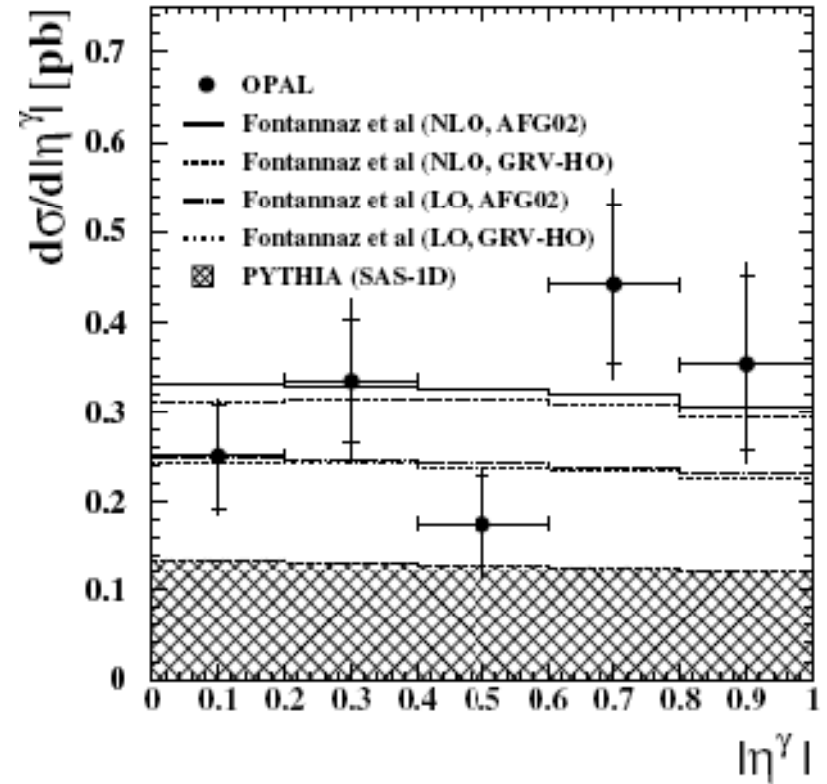
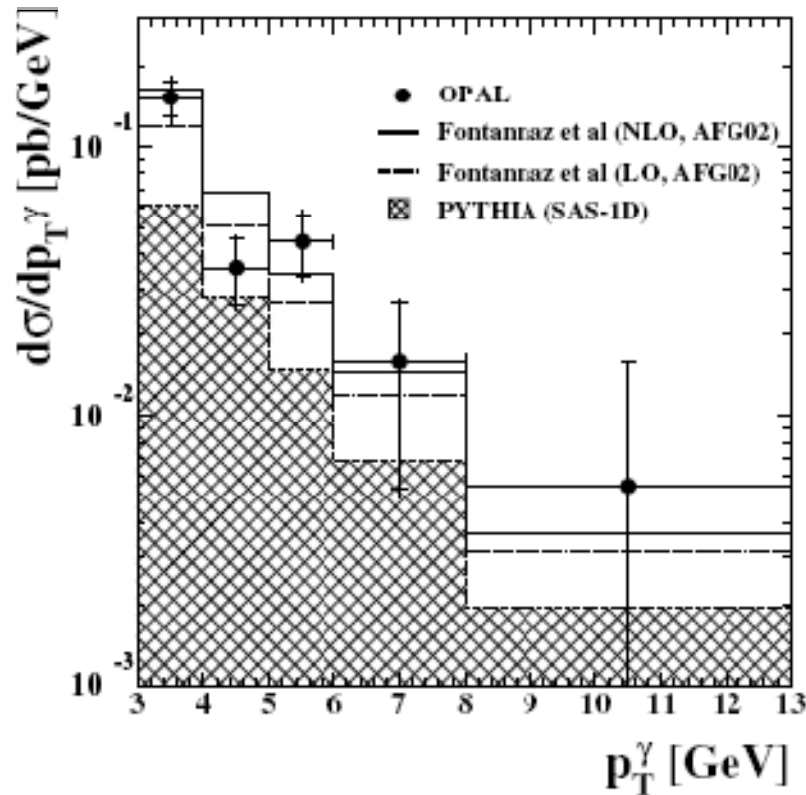
Direct with FSR

Small cross section, but also small hadronisation corrections!

Total cross section in the kinematic range defined by anti-tagging condition, measured by OPAL at $\sqrt{s_{ee}}=183\text{-}209$ GeV:

$$\sigma_{\text{tot}} = 0.32 \pm 0.04(\text{stat}) \pm 0.04(\text{sys})$$

Differential cross sections for $\gamma+\gamma \rightarrow \gamma+X$

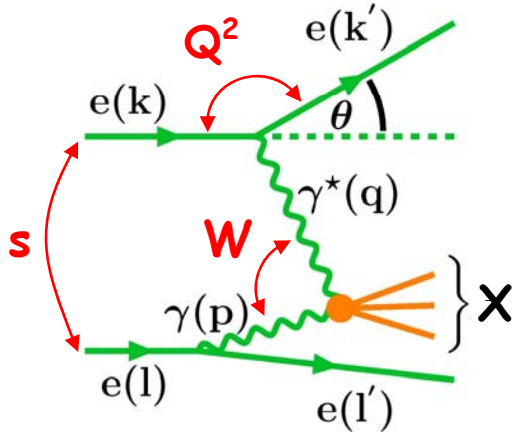


Cross sections measured in the kinematic range $|\eta^\gamma| < 1$ and $p_T^\gamma > 3$ GeV

- Pythia reproduces the shape of the distributions well, but underestimate the normalisation.
- NLO calculations describe well shape and normalisation.

Kinematics of e-γ and e-e DIS

e-γ DIS



$$s = (\mathbf{k} + \mathbf{l})^2$$

$$W^2 = (\mathbf{p} + \mathbf{q})^2$$

s : e^+e^- cms energy squared
 W^2 : $\gamma^*-\gamma$ cms energy squared

$$Q^2 \equiv -\mathbf{q}^2 = -(\mathbf{k} - \mathbf{k}')^2 > 0$$

$$P^2 \equiv -\mathbf{p}^2 = -(\mathbf{l} - \mathbf{l}')^2 \approx 0$$

Q^2 : virtuality of the probe photon
 P^2 : virtuality of the target photon

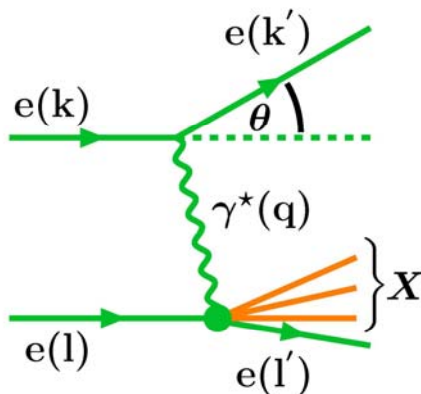
$$y_e = \frac{\mathbf{l} \cdot \mathbf{q}}{\mathbf{l} \cdot \mathbf{k}}$$

$$x = \frac{Q^2}{2\mathbf{p} \cdot \mathbf{q}}$$

$$z = \frac{Q^2}{2\mathbf{l} \cdot \mathbf{q}}$$

y_e : inelasticity, fraction of the elec. mom carried by the virtual photon
 x : fraction of the target photon mom carried by the struck parton
 z : fraction of the target electron mom carried by the struck parton

e-e DIS



$$Q^2 = 2E'E_b(1 - \cos \theta)$$

$$W^2 = (\sum_h E_h)^2 - (\sum_h \vec{p}_h)^2$$

$$y_e = 1 - \frac{E}{E_b} \cos^2(\theta/2)$$

$$x = \frac{Q^2}{Q^2 + W^2 + P^2}$$

$$z = \frac{Q^2}{y_e s}$$

Reconstruction of the kinematical variables is based on the measurement of the scattered electron and the hadronic final state:

Cross section for $e^+e^- \rightarrow e^+e^-\gamma^* \rightarrow e^+e^-X$

The cross section in terms of the photon structure functions F_2^γ and F_L^γ :

$$\frac{d^4\sigma_{ee}}{dx dQ^2 dz dP^2} = \frac{2\pi\alpha^2}{x^2 Q^4} \left[\left(1 + (1 - y_e)^2\right) F_2^\gamma(x, Q^2, P^2) - y_e^2 F_L^\gamma(x, Q^2, P^2) \right] \hat{f}_{\gamma/e}(z/x, P^2)$$

where the flux of (transverse) quasi-real photons given by EPA reads:

$$\hat{f}_{\gamma/e}(y, P^2) = \frac{\alpha}{2\pi} \frac{1}{P^2} \left[\frac{1 + (1 - y)^2}{y} - 2y \frac{m_e^2}{P^2} \right]$$

$$P_{\min}^2(y) = \frac{m_e^2 y^2}{1 - y}$$

$$P_{\max}^2(y) = (1 - y) E^2 \theta_{\max}^2$$

Integrating over z and P^2 we obtain:

$$\frac{d^2\sigma_{ee}}{dx dQ^2} \approx \frac{2\pi\alpha^2}{x Q^4} F_2^\gamma(x, Q^2, P_{\text{eff}}^2) \mathbf{K} \left(\frac{Q^2}{xs}, \frac{P_{\max}^2}{m_e^2} \right)$$

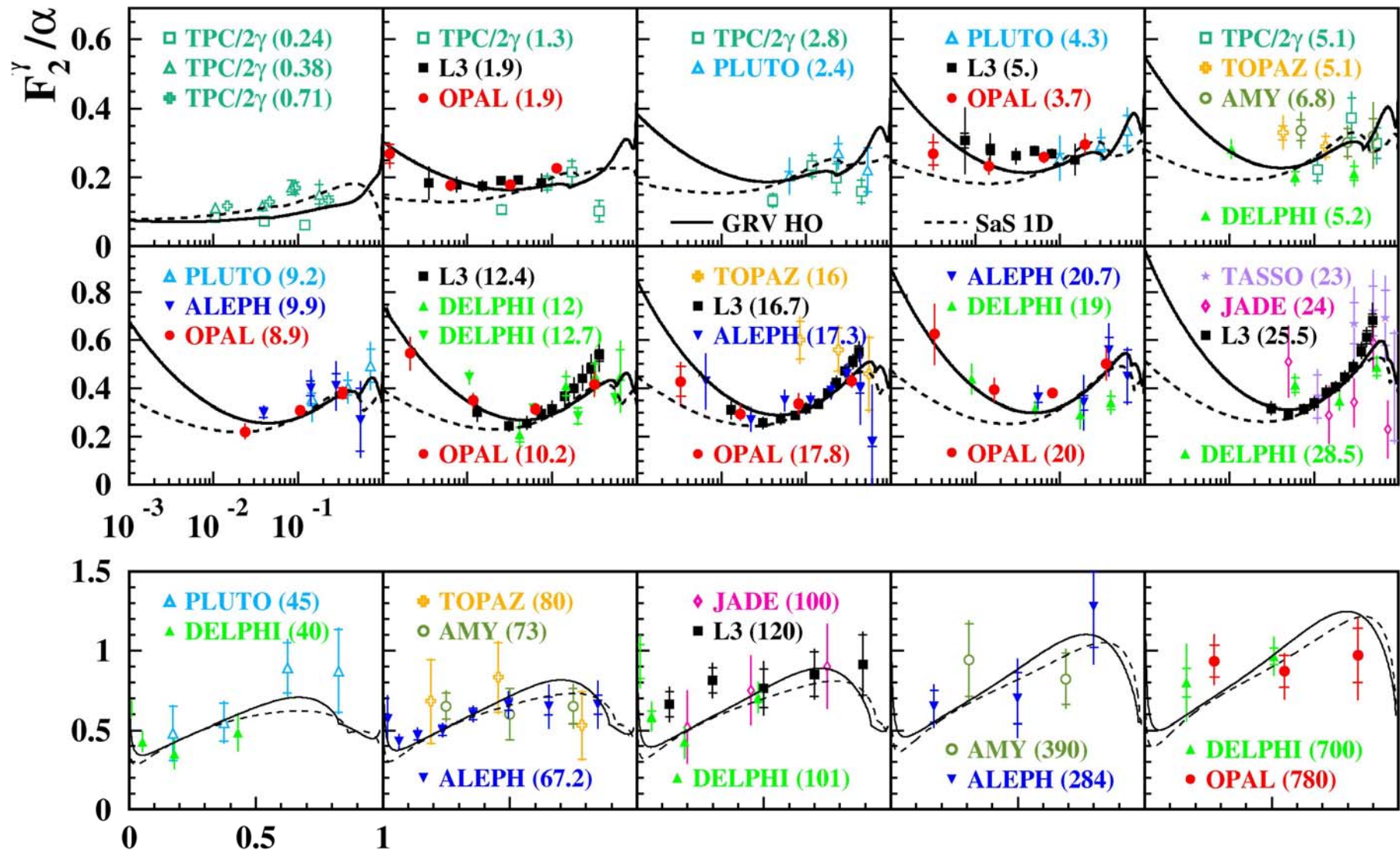
$$\langle F_2^\gamma(P^2) \rangle = F_2^\gamma(P_{\text{eff}}^2)$$

Usually the formula for the cross section for the process $e\gamma \rightarrow eX$ is used for extraction of the F_2^γ based on MC and known input pdf:

$$\frac{d^2\sigma_{e\gamma}}{dx dQ^2} = \frac{2\pi\alpha^2}{x Q^4} \left[\left(1 + (1 - y_e)^2\right) F_2^\gamma(x, Q^2, P_{\text{eff}}^2) \right]$$

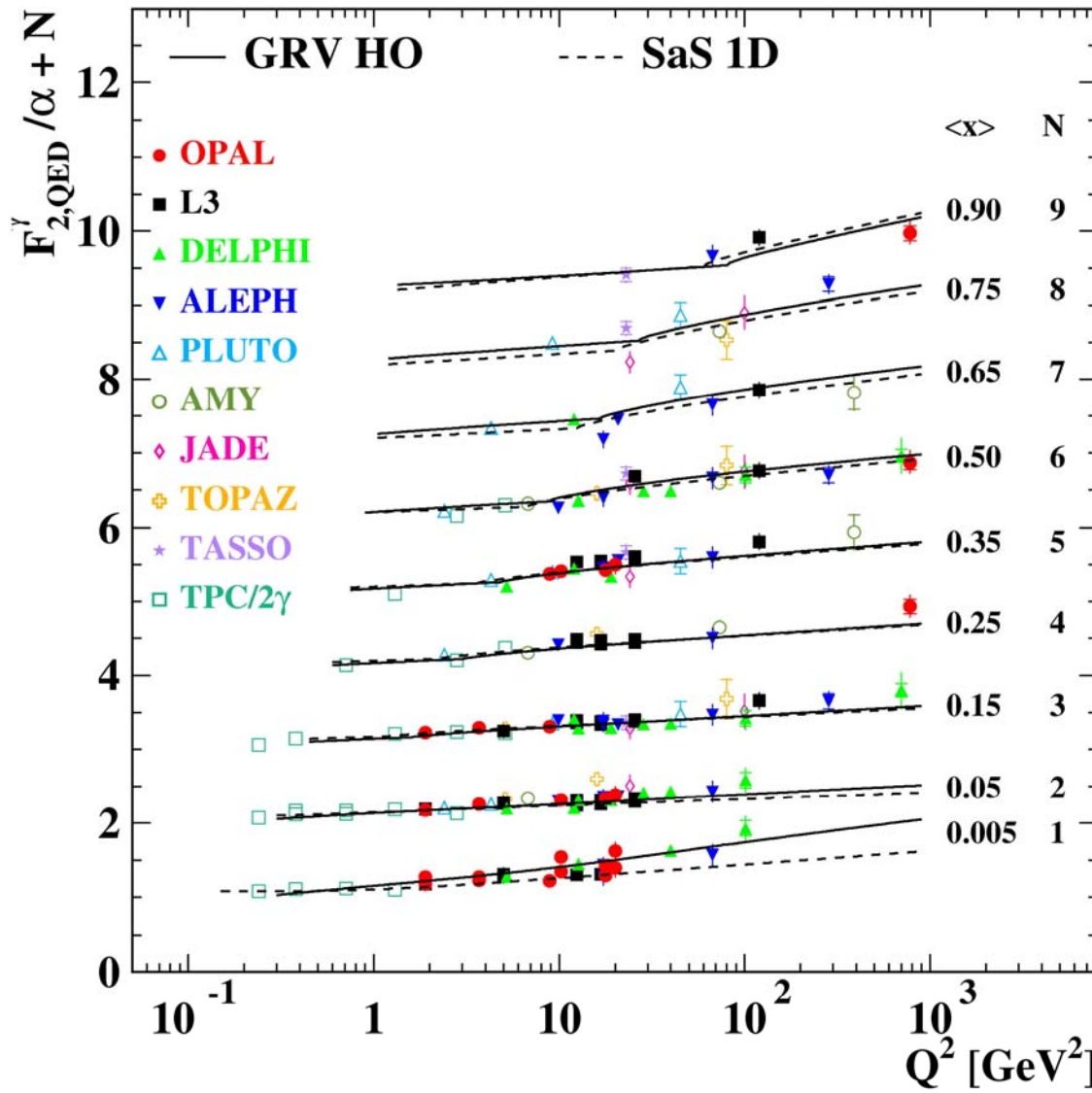
usually we
assume $P_{\text{eff}}^2 = 0$

World data on F_2^γ vs. x



X

World data on F_2^γ vs. Q^2



About 50 measurements

Kinematical range:

$$10^{-3} \leq x \leq 0.9$$

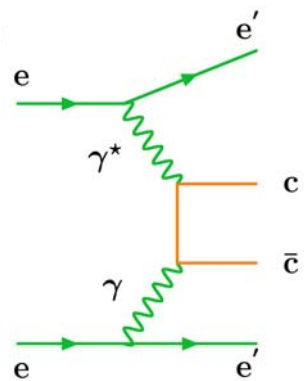
$$1.9 \leq \langle Q^2 \rangle \leq 780 \text{ GeV}^2$$

Good agreement between experiments

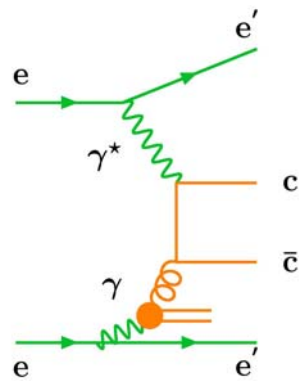
Significant hadron-like component

Positive scaling violation in whole x range (significant increase of the slope with increasing x)

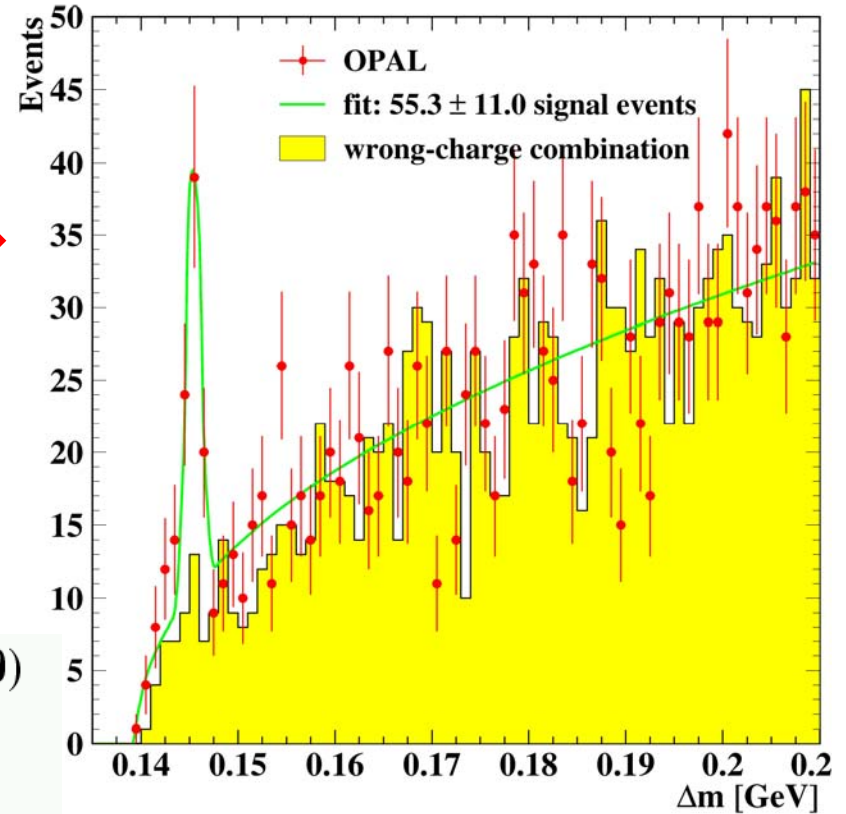
Measurement of F_2^{charm}



Point-like part
(pQCD)



Hadron-like part
depends on gluon
in the photon



$\mathcal{L} = 654.1 \text{ pb}^{-1}$ at 183 – 209 GeV (1997 – 2000)

$\langle \sqrt{s_{ee}} \rangle = 196.6 \text{ GeV}$

$5 < Q^2 < 100 \text{ GeV}^2$, $\langle Q^2 \rangle \approx 20 \text{ GeV}^2$

55.3 ± 11.0 events

$x < 0.1$: 23.6 ± 7.4 events

$x > 0.1$: 31.4 ± 8.1 events

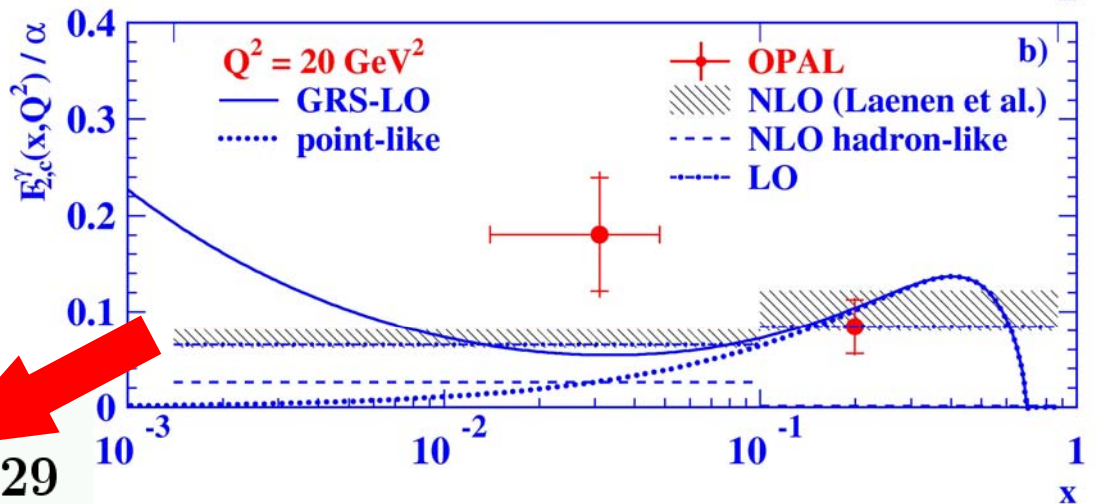
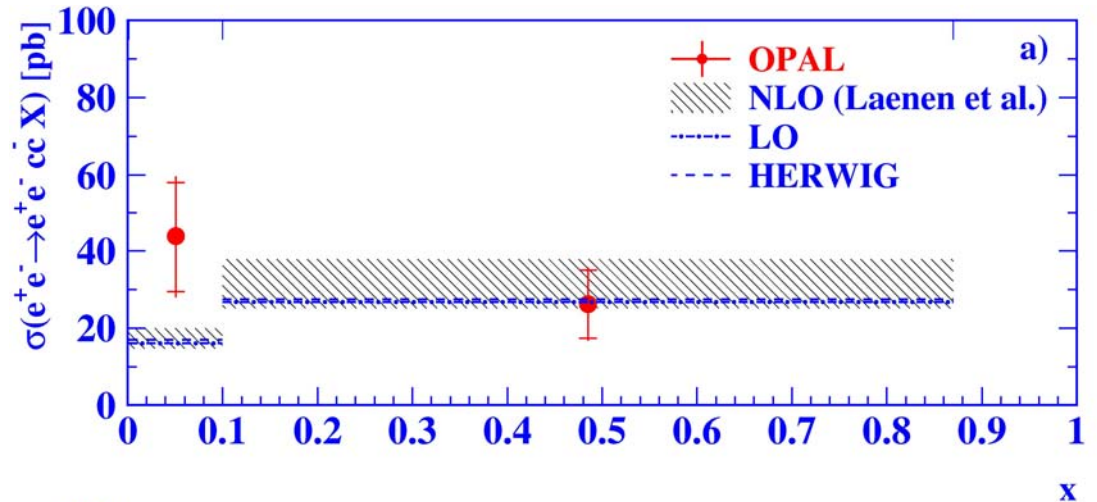
Δm - mass difference of
 $D^{\Sigma+} \rightarrow D^0 p^+$ and $D^0 \rightarrow K^- \pi^+ (\pi^- \pi^+)$

Measurement of F_2^{charm}

Limited by statistics

High- x :
well described by pQCD
calculation, essentially
pointlike

Low- x :
somewhat higher than
predicted, but large error



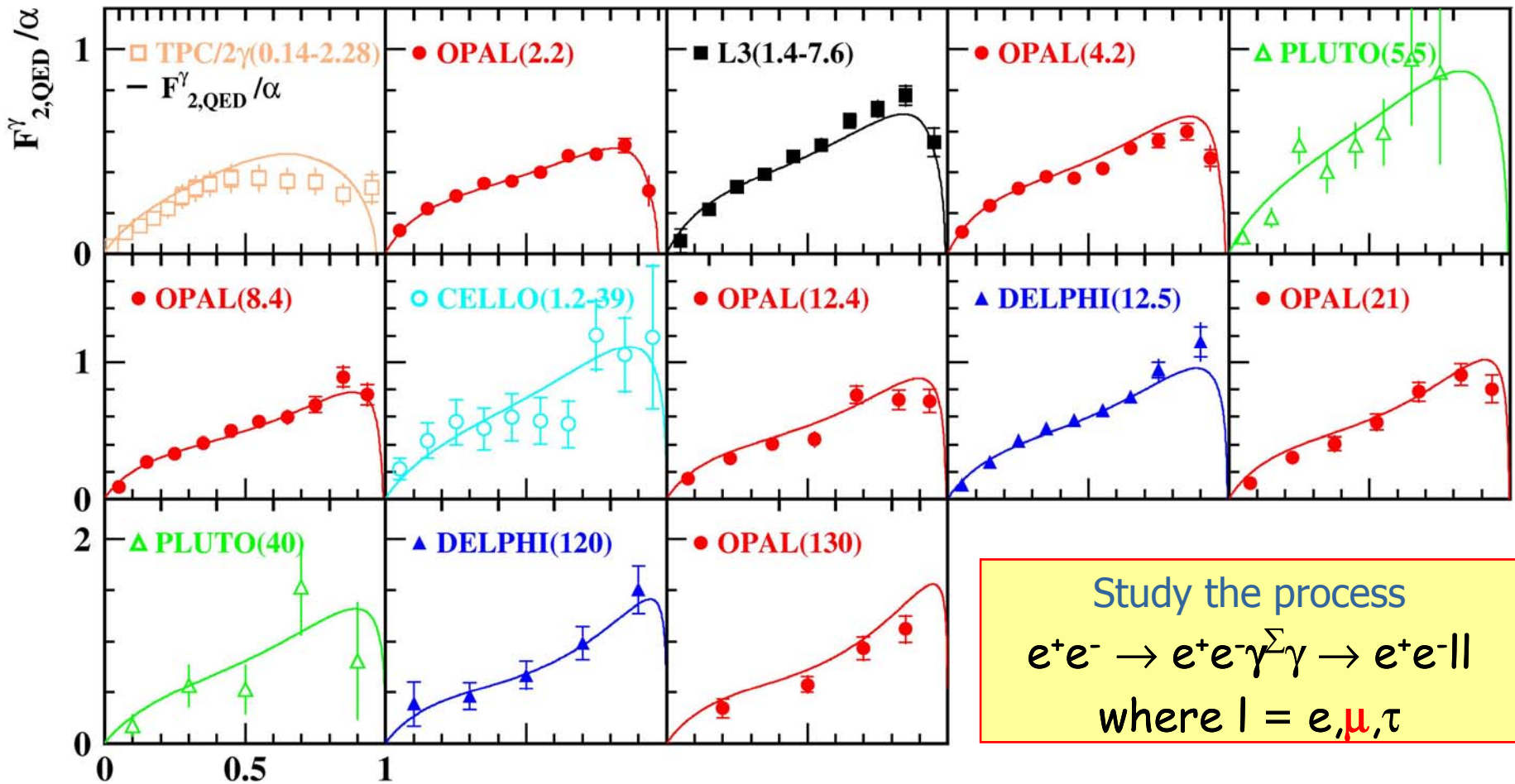
Subtract NLO pointlike part
at low x we obtain:

$$F_{2,c}^{\gamma, \text{HL}} = 0.136 \pm 0.059 \pm 0.029$$

$$\text{NLO prediction: } 0.026^{+0.007}_{-0.005}$$

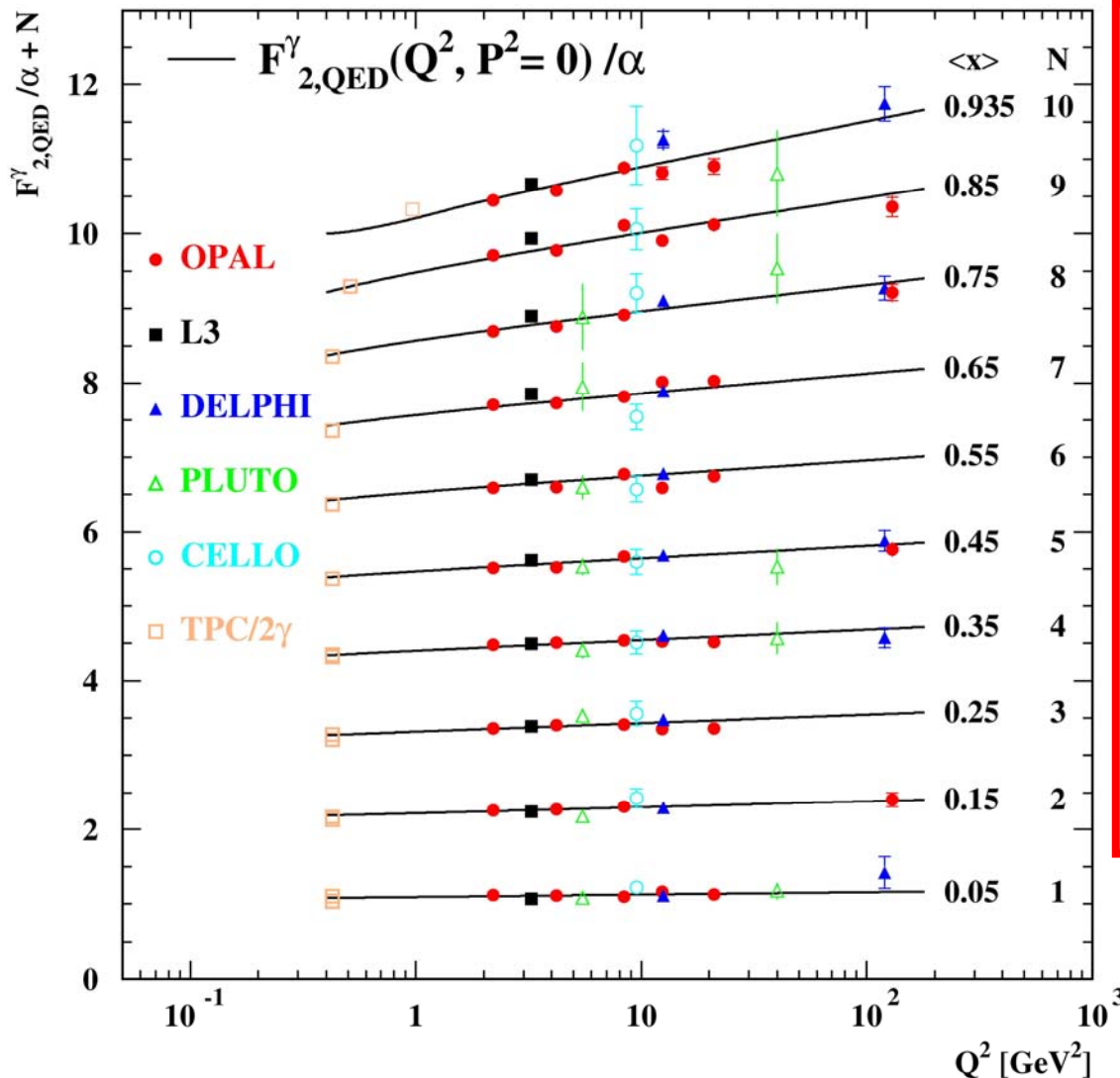
Hadron-like component of $F_{2,c}^{\gamma}$ is needed

World data on $F_{2,QED}^\gamma$ vs. x



$$\frac{d^2\sigma_{e\gamma \rightarrow e\mu^+\mu^-}}{dx dQ^2} = \frac{2\pi\alpha^2}{xQ^4} \left[\left(1 + (1 - y_e)^2\right) F_{2,QED}^\gamma(x, Q^2, P^2) - y_e^2 F_{L,QED}^\gamma(x, Q^2, P^2) \right]$$

World data on $F_{2,QED}^\gamma$ vs. Q^2



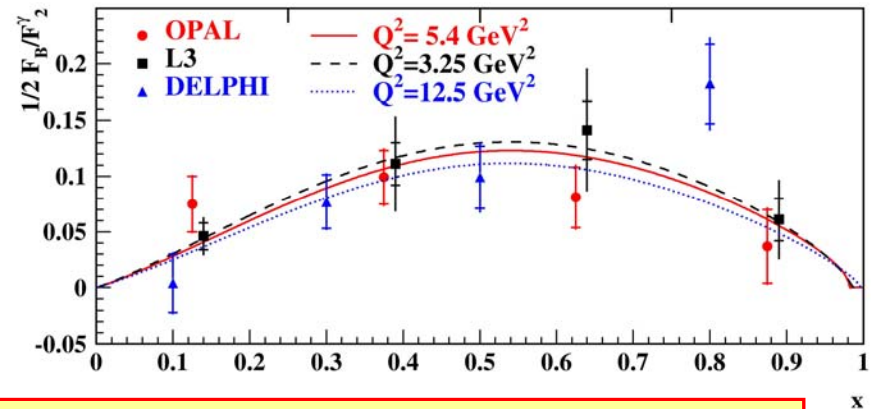
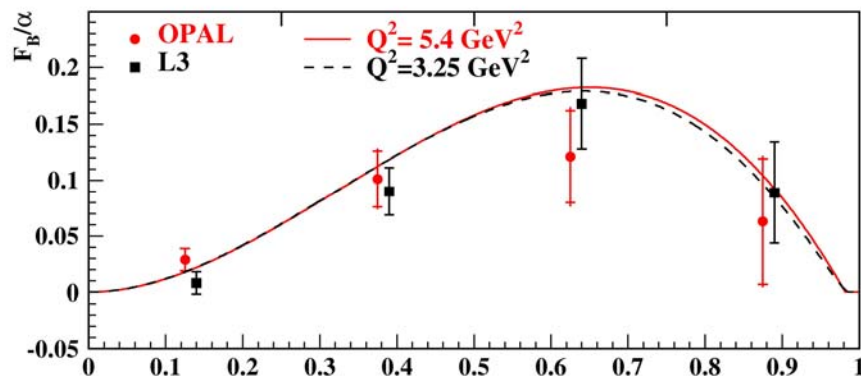
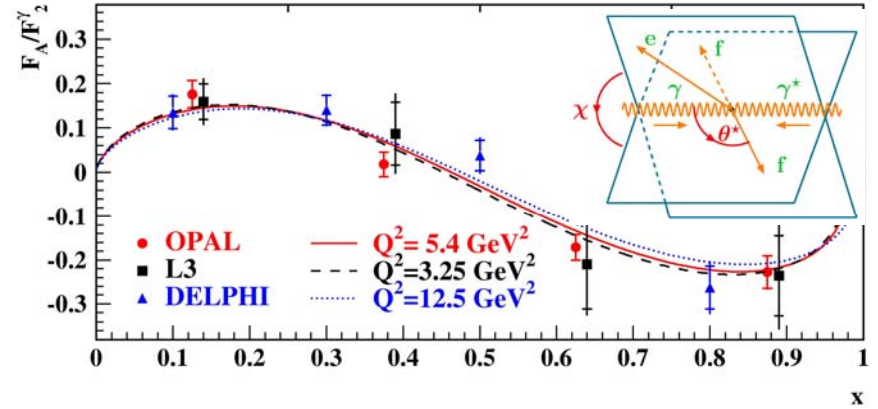
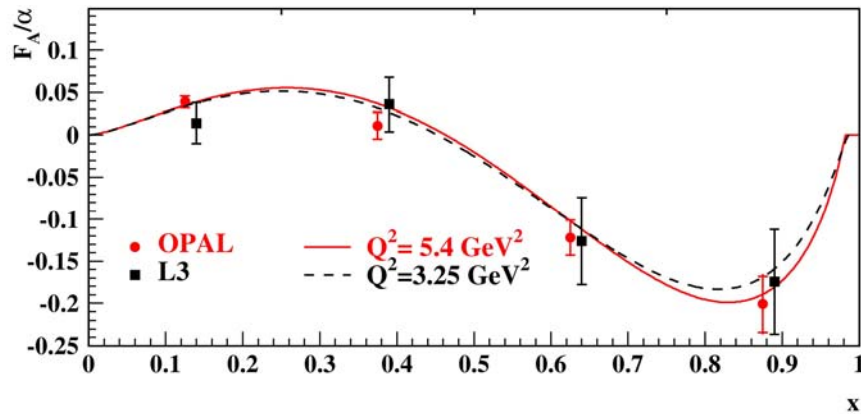
All data points with known P^2 are corrected to $P^2=0$

If for a particular data set the range of Q^2 is given, then for each data point at given x a separate average value of Q^2 has been calculated (TPC/2 γ)

Data clearly follow increasing slope with increasing x

$$0.43 < \langle Q^2 \rangle < 130 \text{ GeV}^2$$

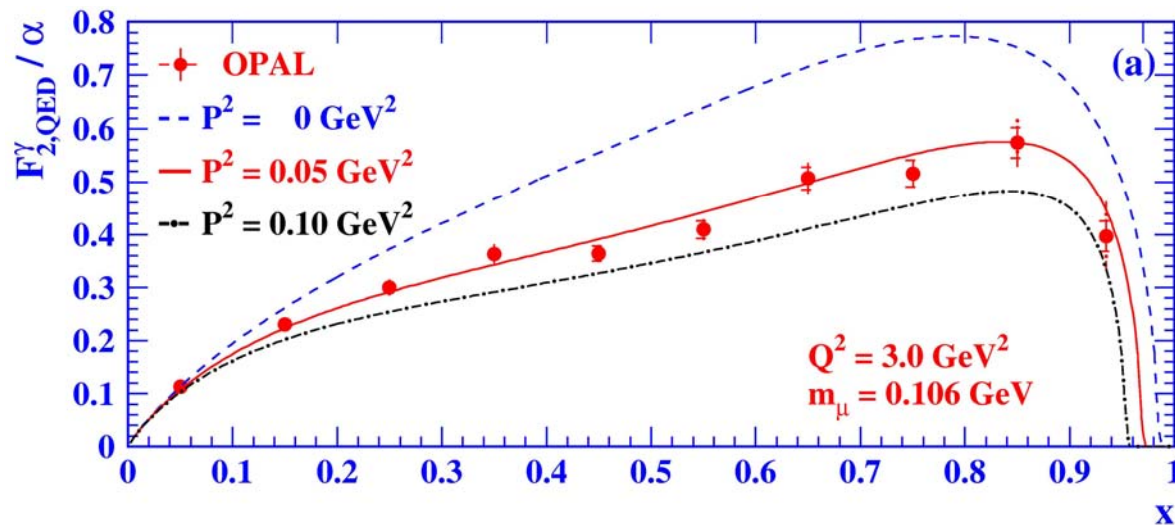
QED structure of the photon



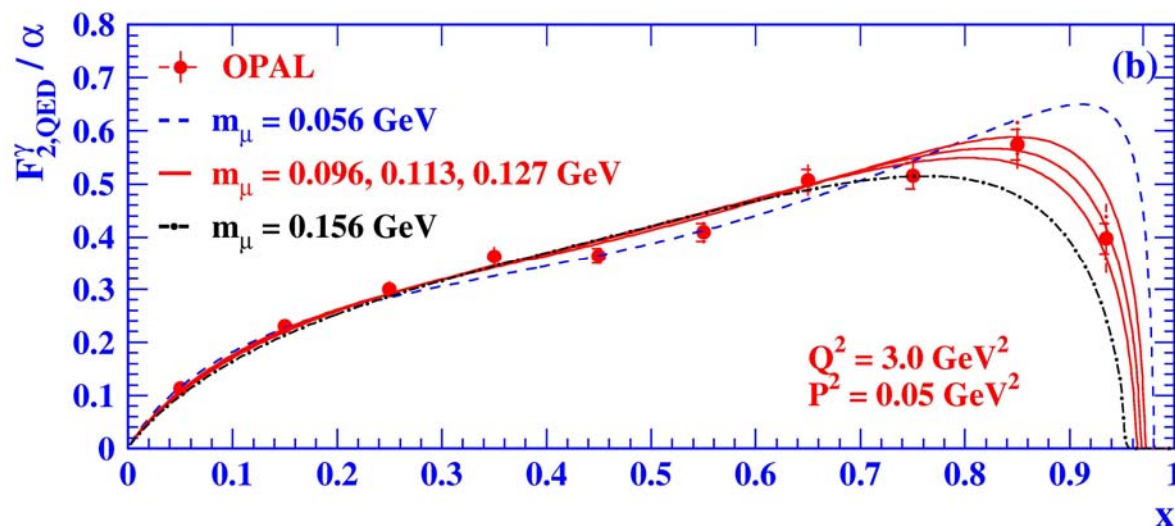
$$\frac{d^3\sigma_{e\gamma\rightarrow\text{eff}}}{dx dQ^2 d\chi/2\pi} \approx \frac{2\pi\alpha^2}{xQ^4} (1 + (1 - y_e)^2) \left[F_{2,\text{QED}}^\gamma(x, Q^2) - F_{A,\text{QED}}^\gamma \cos\chi + \frac{1}{2} F_{B,\text{QED}}^\gamma \cos 2\chi \right]$$

Experimentally verified that both F_A^γ and F_B^γ are different from zero and not constant (const fit: $F_B^\gamma/\alpha = 0.032$ (0.034) OPAL (L3) with $\chi^2/\text{ndf} = 8.9$ (3.1))

Precision of QED measurements



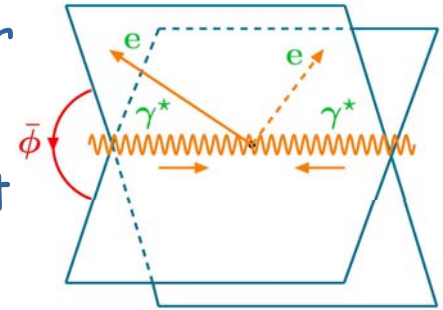
Data are precise enough to observe the effect of small virtuality P^2 of the quasi-real target photon.



From the fit to the data the mass of the muon can be measured with precision of about 14%.

Interactions of virtual photons

The general form of the differential cross section for the process $e(p_1)e(p_2) \rightarrow e(p_1')e(p_2')X$ which proceeds via the exchange of two photons $\gamma(q_1), \gamma(q_2)$ in the limit $Q_i^2 \gg m_e^2$, is given by:



$$d^6\sigma = \frac{d^3 p_1' d^3 p_2'}{E_1' E_2'} \frac{\alpha^2}{16\pi^4 q_1^2 q_2^2} \left[\frac{(q_1 \cdot q_2)^2 - q_1^2 q_2^2}{(p_1 \cdot p_2)^2 - m_e^2 m_e^2} \right]^{1/2} 4\rho_1^{++} \rho_2^{++} \cdot$$

$$\cdot \left(\sigma_{\text{TT}} + \varepsilon_1 \sigma_{\text{LT}} + \varepsilon_2 \sigma_{\text{TL}} + \varepsilon_1 \varepsilon_2 \sigma_{\text{LL}} + \frac{1}{2} \varepsilon_1 \varepsilon_2 \tau_{\text{TT}} \cos 2\bar{\phi} - 2\sqrt{\varepsilon_1(1+\varepsilon_1)}\sqrt{\varepsilon_2(1+\varepsilon_2)}\tau_{\text{TL}} \cos \bar{\phi} \right)$$

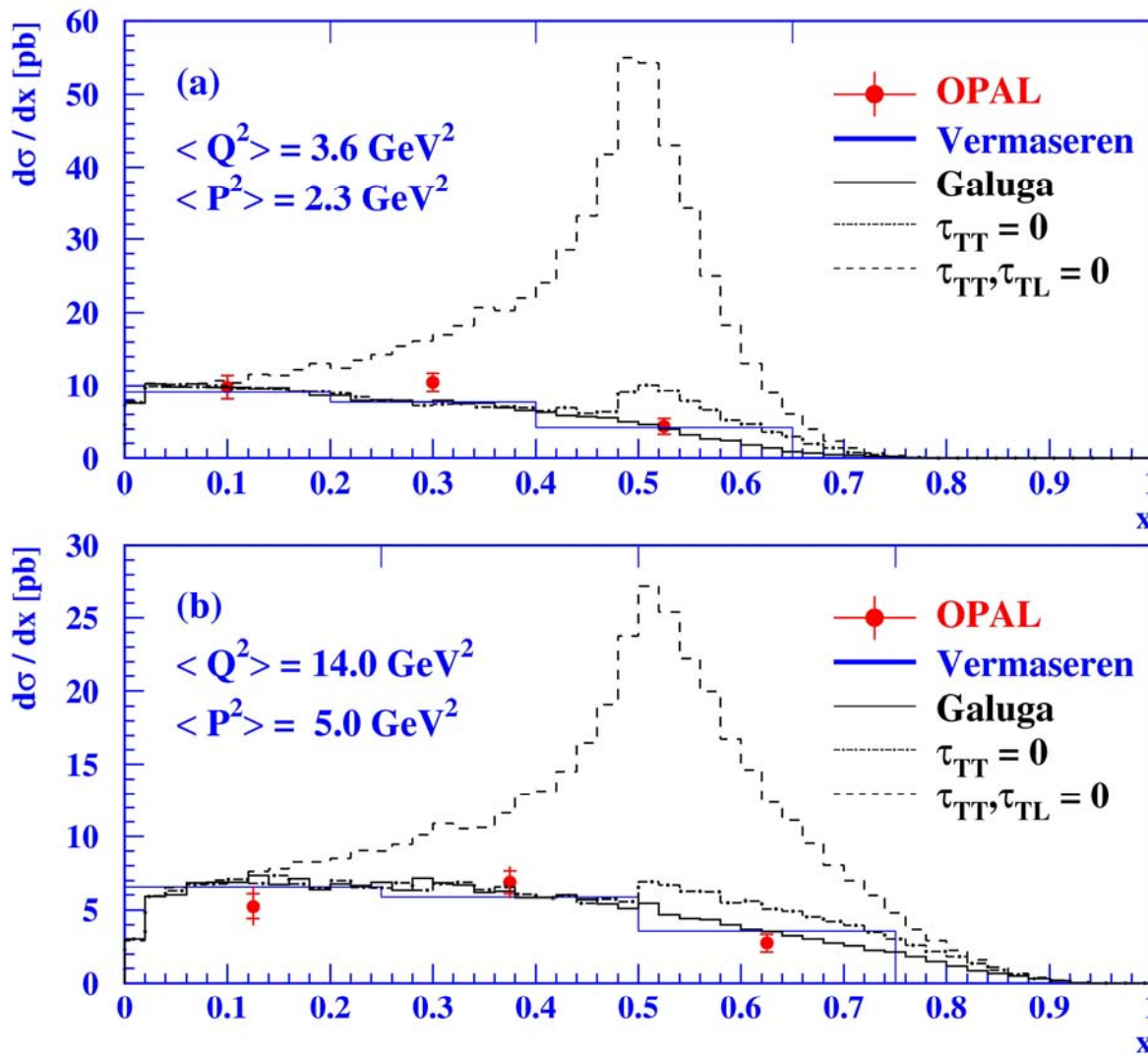
Introducing the luminosity function, we define the cross section for the scattering of two virtual photons $\gamma^\Sigma \gamma^\Sigma \rightarrow X$:

$$d^6\sigma = \frac{d^3 p_1' d^3 p_2'}{E_1' E_2'} L_{\text{TT}} \sigma_{\gamma^* \gamma^*}$$

$$\sigma_{\gamma^* \gamma^*} = \sigma_{\text{TT}} + \sigma_{\text{LT}} + \sigma_{\text{TL}} + \sigma_{\text{LL}} + \frac{1}{2} \tau_{\text{TT}} \cos 2\bar{\phi} - 4\tau_{\text{TL}} \cos \bar{\phi}$$

$$L_{\text{TT}} = \frac{d^3 p_1' d^3 p_2'}{E_1' E_2'} L_{\text{TT}}$$

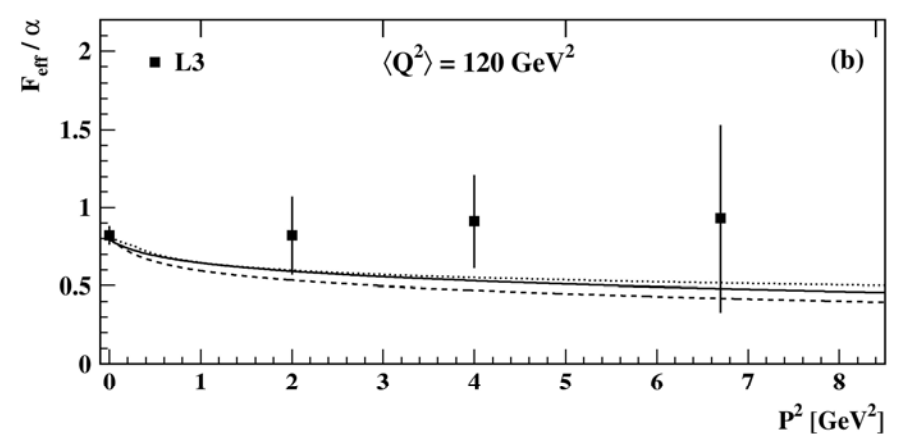
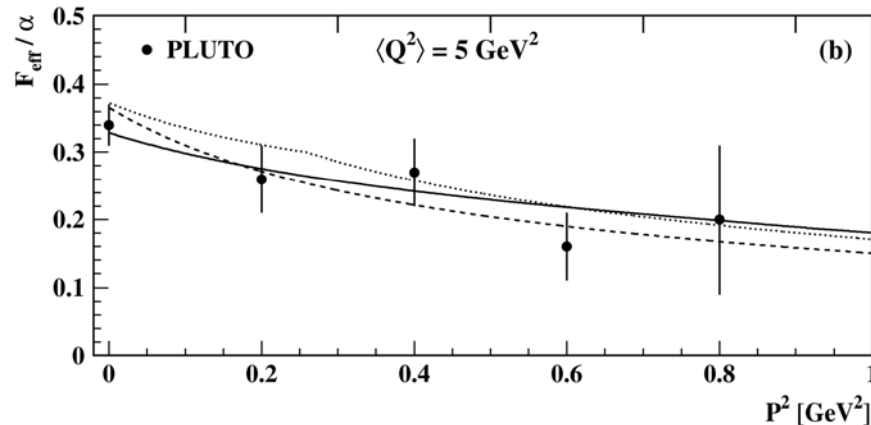
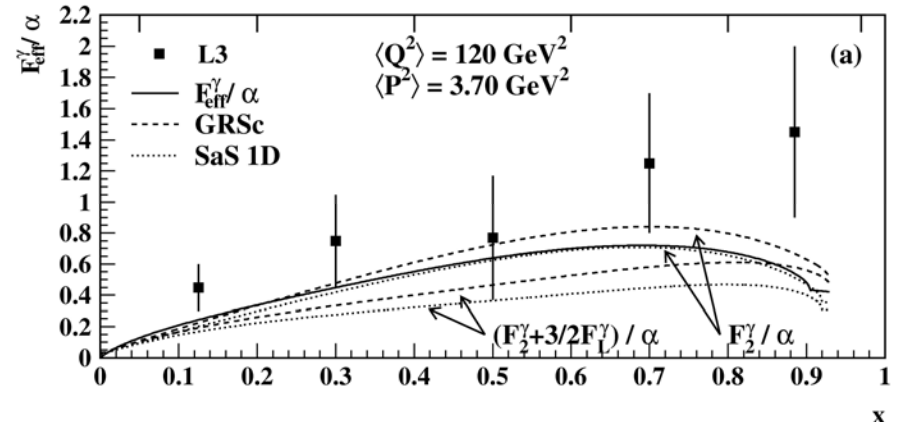
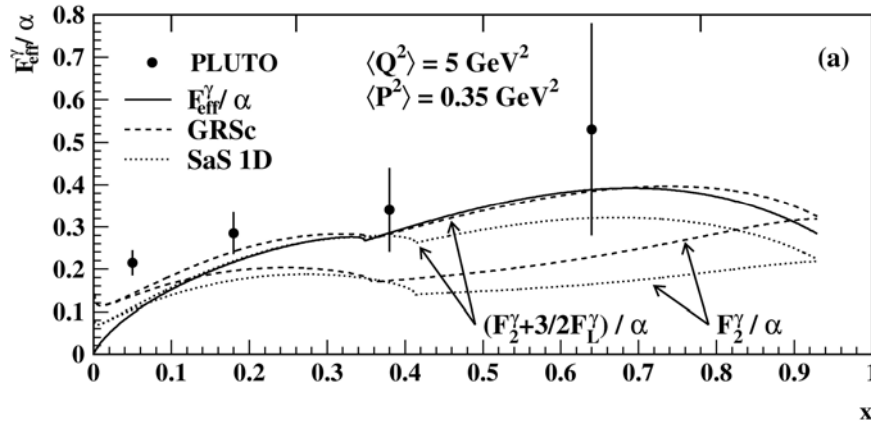
QED structure of the virtual photon



Data are well described by the predictions of programs based on the full cross section formula.

It is clearly seen that the terms τ_{TT} and τ_{TL} are present mainly at $x > 0.1$

Structure function of virtual photon



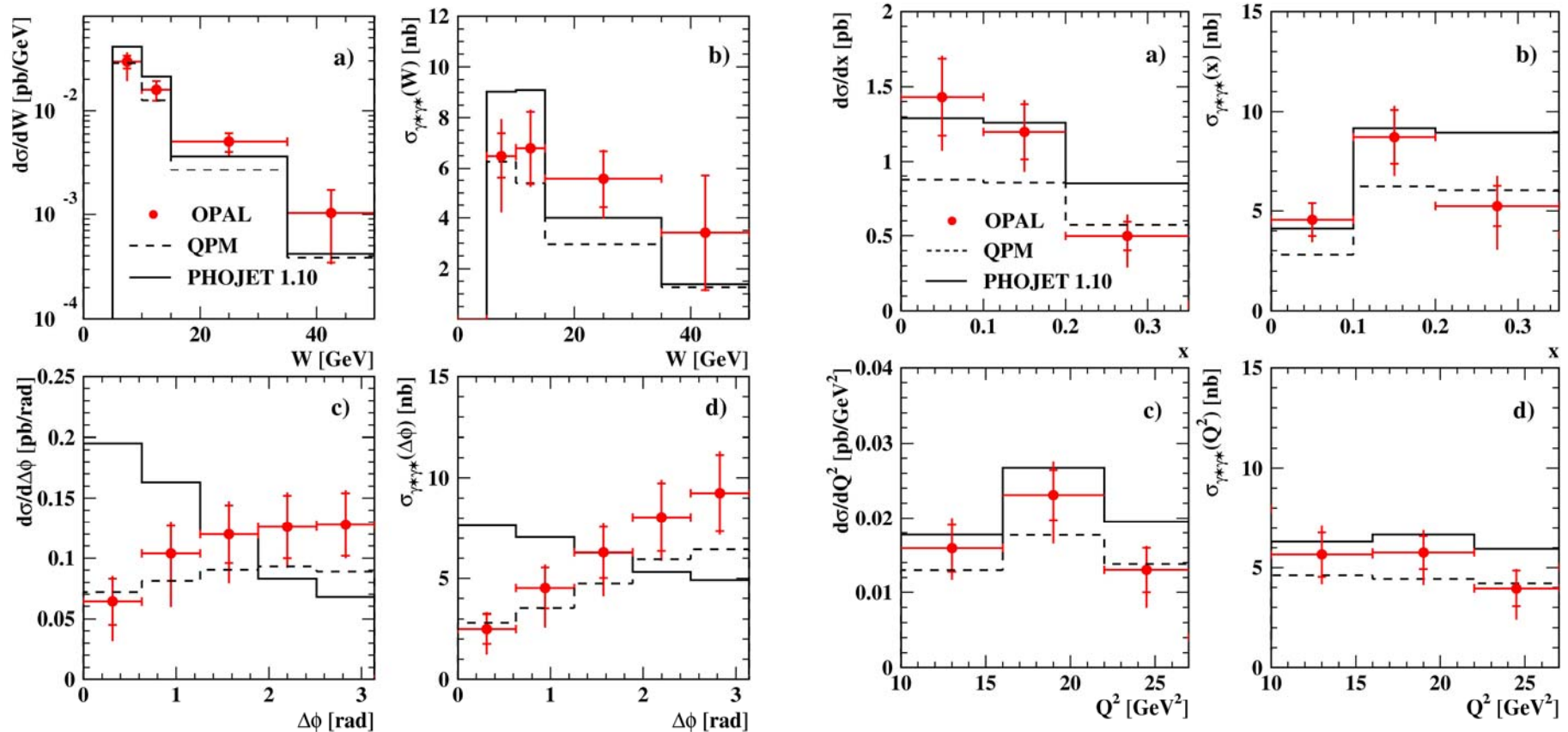
Experimentally one can access only an effective structure function:

$$F_{\text{eff}}^\gamma \square \sigma_{\gamma^* \gamma^*} \quad F_{\text{eff}}^\gamma \square F_2^\gamma + \frac{3}{2} F_L^\gamma$$

Good agreement within statistical errors with QPM predictions.

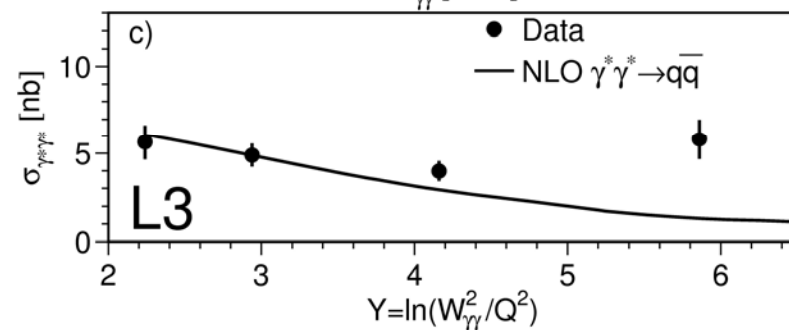
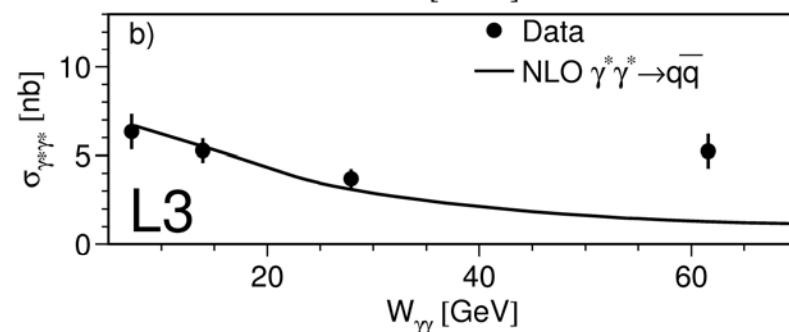
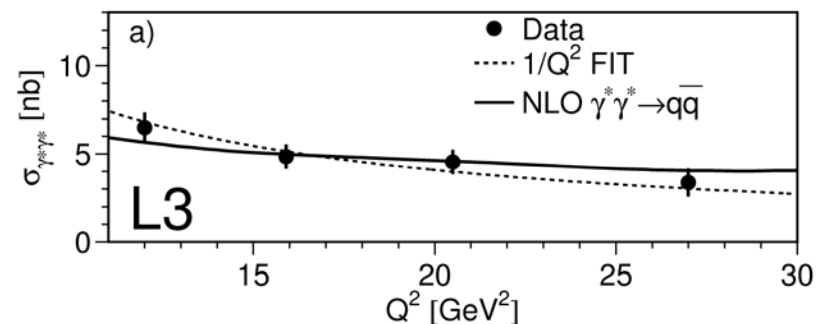
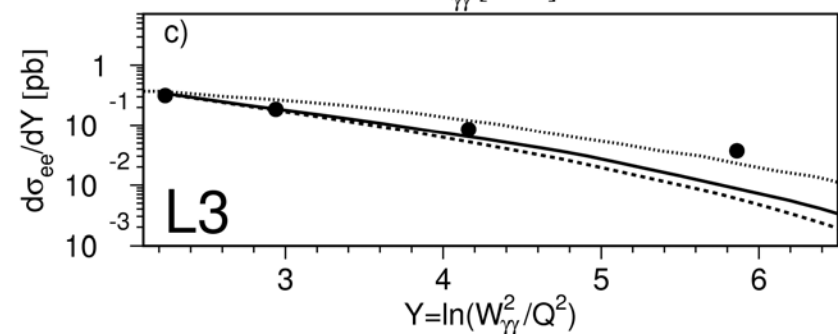
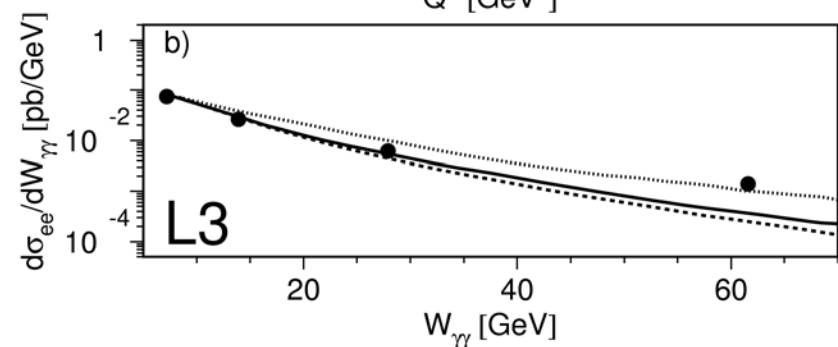
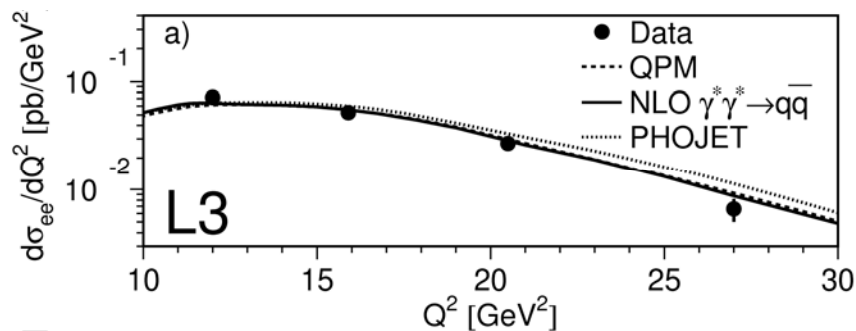
PLUTO data suggest, as expected slow decrease with increasing P^2

Structure of virtual photon interactions

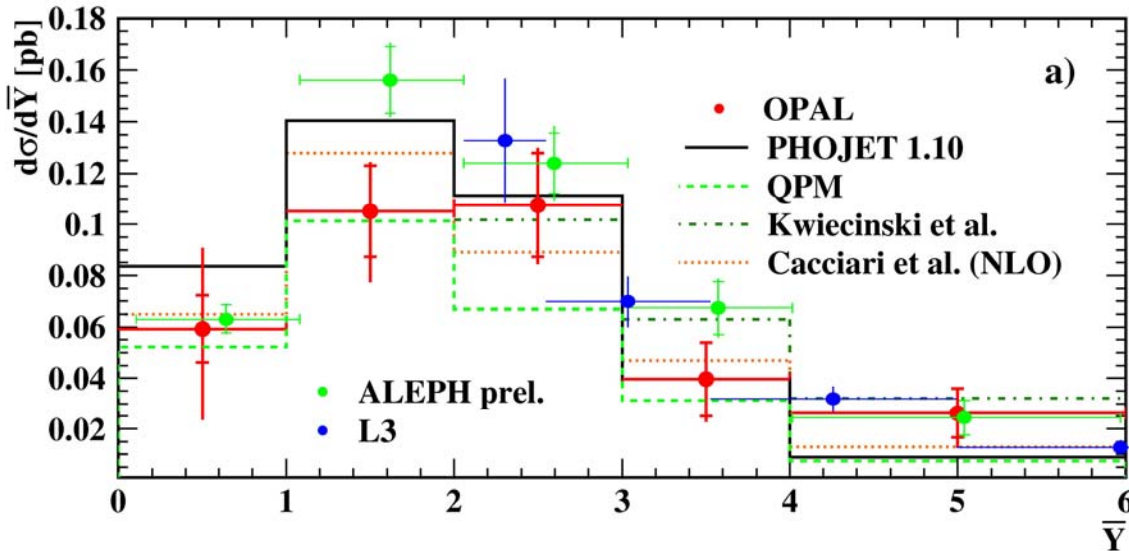


Cross sections for the processes $e^+e^- \rightarrow e^+e^- \text{hadrons}$ and $\gamma^*\gamma^* \rightarrow \text{hadrons}$, in the phase space region $E_i > 0.4E_b$, $34 < \theta_i < 55$ mrad, $W > 5$ GeV; $\langle Q^2 \rangle = 17.9$ GeV²

Scattering of virtual photons



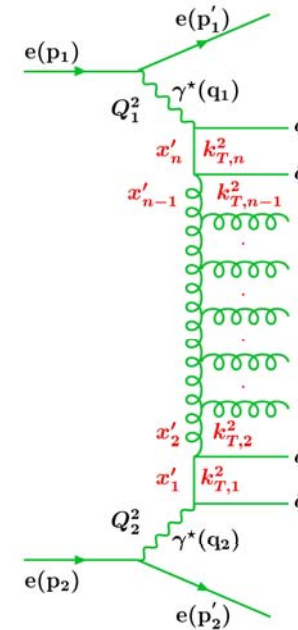
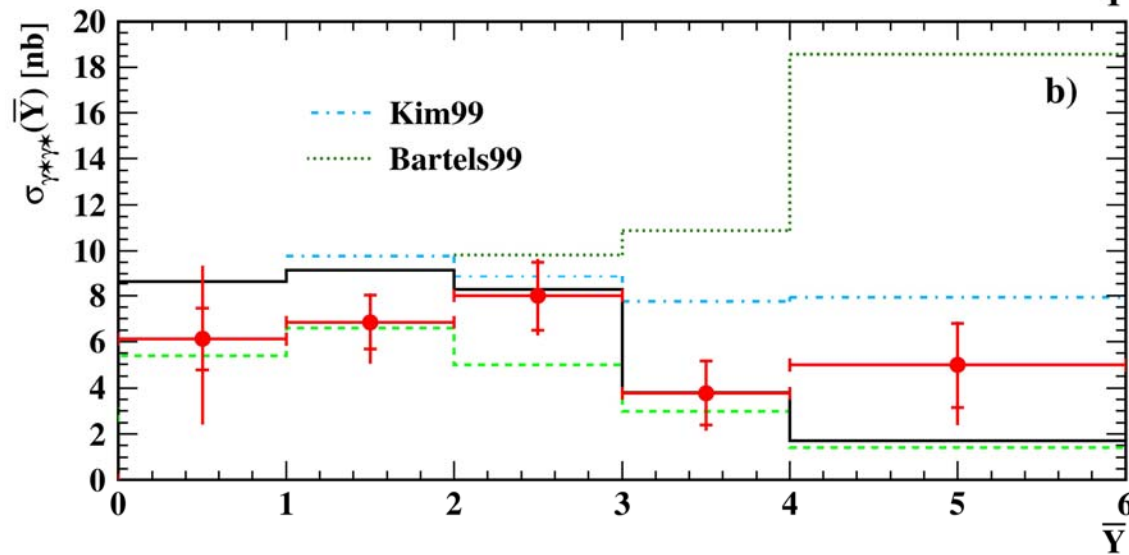
Dynamics of interactions of virtual photons



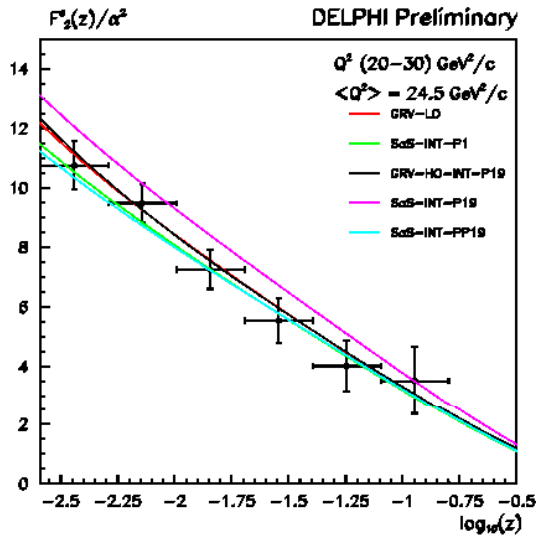
For comparison with BFKL calculations

$$Y \equiv \ln \left(\frac{s_{ee} y_1 y_2}{\sqrt{Q_1^2 Q_2^2}} \right) \approx$$

$$\approx \ln \left(\frac{W^2}{\sqrt{Q_1^2 Q_2^2}} \right) \equiv \bar{Y}$$



Electron structure function

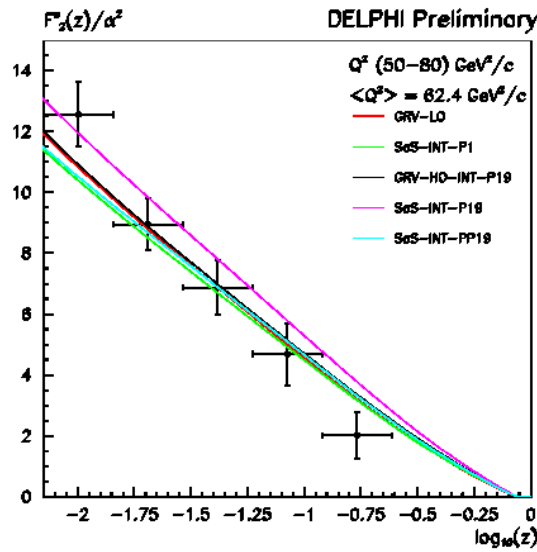
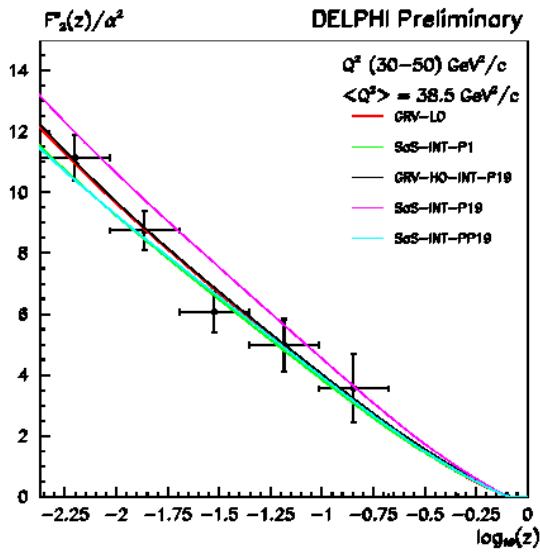


Cross section in terms of electron structure functions:

$$\frac{d^2\sigma_{ee}}{dzdQ^2 dzdP^2} = \frac{2\pi\alpha^2}{zQ^4} \left[\left(1 + (1 - y_e)^2\right) F_2^e(z, Q^2) - y_e^2 F_L^e(z, Q^2) \right]$$

Photon and electron structure functions are related:

$$F_a^e(z, Q^2; P_{\max}^2) \equiv \int_z^1 dx \int_{P_{\min}^2(z/x)}^{P_{\max}^2} dP^2 \frac{z}{x^2} F_a^\gamma(x, Q^2, P^2) \hat{f}_{\gamma/e}(z/x, P^2)$$



- unknown P^2 of target γ
- F^e do not depends on the form of equivalent photon formula
- shape dominated by strongly peaked flux of target photons

Summary

LEP2 - the best place to study two photon interactions:

~100 published papers from all four experiments (mainly from LEP2)

Untagged measurements:

- total cross section
- jet and di-jet production
- production of resonances, charged hadrons, prompt photons, charm and beauty

Single tagged measurements:

- QED and hadronic structure functions of the quasi-real photon

Double tagged measurements:

- QED and hadronic structure of interactions of virtual photons
- total and differential cross sections and effective structure function of the virtual photon

More about tagged measurements in <http://home.agh.edu.pl/mariuszp>